PCCP

Cite this: *Phys. Chem. Chem. Phys.*, 2011, **13**, 16680–16688

www.rsc.org/pccp

PAPER

Surface models and reaction barrier in Eley–Rideal formation of H_2 on graphitic surfaces

Matteo Bonfanti,[a] Simone Casolo,[a] Gian Franco Tantardini[ab] and Rocco Martinazzo*[a]

Received 10th June 2011, Accepted 26th July 2011
DOI: 10.1039/c1cp21900f

The exothermic, collinearly-dominated Eley–Rideal hydrogen formation on graphite is studied with electronic structure and quantum dynamical means. In particular, the focus is on the importance of the model used to describe the graphitic substrate, in light of the marked discrepancies present in available literature results. To this end, the collinear reaction is considered and the potential energy surface is computed for a number of different graphitic surface models using Density Functional Theory (DFT) for different dynamical regimes. Quantum dynamics is performed with wavepacket techniques down to the cold collision energies relevant for the chemistry of the interstellar medium. Results show that the reactivity at moderate-to-high collision energies sensitively depends on the shape of the PES in the entrance channel, which in turn is related to the adopted surface model. At low energies we rule out the presence of any barrier to reaction, thereby highlighting the importance of quantum reflection in limiting the reaction efficiency.

1 Introduction

Hydrogen is the most abundant molecule detected in most of the interstellar medium (ISM), *e.g.* in dense and diffuse clouds and in photon-dominated regions, despite hydrogen molecules are continuously dissociated by stellar UV radiation and cosmic rays. An efficient catalytic route for the recombination of atomic hydrogen might take place on the surface of interstellar dust grains, an ensemble of very small particles of different sizes and nature.[1–3] In diffuse clouds, where the intense stellar radiation heats the gas, the largest particles are composed of a silicate core covered by an "organic refractory mantle", whereas smaller particles are entirely carbonaceous, being even simple polycyclic aromatic hydrocarbons.[4–6] Hydrogen formation in these regions of interstellar space may thus occur on graphitic surfaces, and hydrogen–graphite has become the prototypical system for studying hydrogen formation in the ISM. Depending on the physical conditions of interest and on the actual morphology of the surface, a number of formation processes are possible, and only an accurate knowledge of adsorption, diffusion, and recombinative elementary acts allows one to investigate the role of each given pathway and to estimate the corresponding rate constant.

Hydrogen atoms may adsorb on graphitic surfaces either chemically or physically. Physisorbed atoms can only be found in cold environments, since they already desorb at few tens of Kelvins ($T_{des} \approx$ 30–40 K). Tunneling phenomena guarantee a high mobility of H atoms down to vanishing temperatures[7] and, generally, allow hydrogen molecules to form either through a Langmuir–Hinshelwood, or an Eley–Rideal, or a hot-atom mechanism, or a combination of them.[8–10]

The chemisorption process is limited by a significant energy barrier to the sticking process.[11–19] In order to form a covalent bond between the approaching hydrogen atom and a carbon atom of the graphite (0001) surface, it is required that the carbon's sp^2 orbitals rehybridize to a tetrahedral sp^3 state. This process introduces a substantial lattice reconstruction, with one carbon atom moving out of the surface plane by about 0.35 Å, thereby causing a surface "puckering". As a consequence, a barrier to chemisorption of $\sim$0.15 eV (1700 K) high appears, and essentially prevents (direct) hydrogen sticking in the chemisorption well at temperatures typical of the ISM (T = 10–100 K in diffuse clouds). For this reason, direct chemisorption of H atoms is expected to take place only in photon dominated or shocked regions where the temperature is high enough ($T \approx$ 200–1000 K). Nevertheless, chemisorbed H atoms are required in order to explain the observed abundances and have been considered in many reaction mechanisms for hydrogen formation in the ISM.

Recent studies have shown that, due to the peculiar electronic structure of graphite,[20] H atoms tend to cluster already at very low coverages ($\geq$ 1%).[21–24] Molecular formation at high temperatures may thus follow direct recombination of atoms within the clusters (in particular of hydrogen pairs lying in the *para* position of an hexagonal ring[21]) and direct (Eley–Rideal)

[a] *Dipartimento di Chimica Fisica ed Elettrochimica, Università degli Studi di Milano, via Golgi 19, 20133, Milan, Italy. E-mail: rocco.martinazzo@unimi.it*
[b] *CNR-ISTM Institute for Molecular Science and Technology, via Golgi 19, 20133, Milan, Italy*

abstraction may occur on isolated atoms as well as on dimers.[25] In principle, chemisorbed hydrogen atoms can act as catalysts even at low temperature, *e.g. via* the barrierless adsorption of H atoms at their *para* position, followed by direct Eley–Rideal recombination of the latter.[22,25] Langmuir–Hinshelwood reactions, however, are prevented by the lack of mobility of H atoms chemically bound to the surface.

In this work, we focus on the H_2-forming, Eley–Rideal reaction involving a chemisorbed atom and collision energies which reach the *cold* regime ($\sim$1–100 K) where much of the chemistry of the ISM takes place. Many different methodologies and models have been developed to compute the cross section for this process[26–39] but a direct comparison between these studies is hard to perform since different researchers adopted different potential and/or dynamical models. Global differences are, however, already evident under simplified conditions and persist at any level of description. One of them is the behavior of the reaction probability in the collinear geometry when the substrate is kept rigid. As already discussed in ref. 39, some Potential Energy Surfaces (PES) give rise to a sizable reaction probability and to a resonant behavior in the whole energy range 0–0.5 eV,[33] whereas others give rise to a smooth (almost free of resonances) decreasing probability as the energy decreases in the same range.[39] In addition, some authors found a tiny barrier ($\sim$10 meV or, equivalently, $\sim$100 K) in the entrance channel of the reaction and others do not. The existence of such a barrier, of course, has a deep impact on the reaction probability in the astrophysically relevant collision energy regime.

The aim of the present work is to systematically study how the reaction dynamics depends on the model adopted for the graphitic surface. We focus on the collinear reaction and consider how the Potential Energy Surfaces (PES) resulting from different substrate models give rise to different reaction probabilities. Clearly, such reduced dynamical models can only have limited values for the correct description of the title process (and many results concerning these models have been well-known since the birth of the chemical reaction dynamics), but the main focus here is on how the choice of the substrate affects the dynamics. An extension of the model is of course possible but for the present purposes it would be limited by the PES construction. We performed the simulations with quantum dynamical methods, since in the *low* energy regime typical of interstellar conditions the quantum behavior of H atoms cannot be neglected.[39] In addition we perform extensive *first-principles* calculations of the reaction energetics at different theory levels, and definitely rule out the presence of any barrier in the entrance channel of the reaction.

This paper is organized as follows: theoretical methods are presented in Section 2, results are given in Section 3, and conclusions in Section 4.

2 Methodology

The adopted dynamical model is a rigid surface model[40,41] in the collinear geometry, in which the two H atoms lie along a line perpendicular to the surface. The last assumption does not allow us to determine the cross section, which is the relevant observable for the process. However, the reaction is essentially collinearly dominated, and the computed collinear reaction probability can be used to get a clear indication on the reaction cross-sections at different collision energies of the incident H atom. The aim of this investigation is to see whether and how the adopted surface model impacts on the dynamical behavior of the system.

To describe the interaction of the two H atoms with the graphitic surface, we performed Density Functional Theory calculations with different models of the surface. First, we considered a cluster model of graphite (coronene molecule, $C_{24}H_{12}$), a polycyclic aromatic hydrocarbon commonly used for this purpose.[7,15] We computed the interaction energy with the Perdew–Burke–Ernzerhof (PBE) functional[42,43] and Dunning's correlation consistent double ζ basis set (cc-pVDZ),[44] as implemented in GAUSSIAN code.[45] Second, we considered two different periodic models. In this case the graphitic surface is described with a 2×2 or 3×3 graphene supercell; inclusion of additional layers in a slab model does not modify the results significantly, as expected from the large interlayer separation in graphite ($\sim$3.4 Å). The total energy was computed with the PBE functional with the help of the VASP code[46] using a plane waves basis set (with a 500 eV cutoff) and projector augmented wave (PAW) potential for core electrons.[47,48] A vacuum space of 20 Å was placed between graphene layers in order to avoid periodic boundary conditions artifacts and a $15 \times 15 \times 1$ Monkhorst–Pack grid of Γ-centered **k**-points has been used to sample the Brillouin zone.

For each surface model, we considered two limiting dynamical regimes which try to include the lattice motion in the rigid setting.[16,33] In the *sudden model* the position of the carbon atom involved in the CH bond was kept fixed in the puckered geometry; in the (surface) *adiabatic model* the geometry of the carbon atom was optimized for each position of the two reacting H atoms. The first limit is appropriate in the high energy regime, where the reaction is faster than the lattice relaxation, whereas the latter is more adequate at low energies. It should be noticed, though, that neither model can fully take into account the effect of the carbon atom motion, that seems to actively promote the reaction.[33]

For each of the six models described above (coronene cluster, 2×2 and 3×3 periodic supercell in the sudden and in the adiabatic regime) we computed 324 points of the PES as a function of the distances of the two H atoms from the surface, z_i and z_t (Fig. 1), and used 2D splines to have continuous representations of the functions. We used the slope of the *ab initio* data at the edge of the grid to fix the derivatives of the splines, and introduced continuously a long-range tail to the potential of the form $\sim z^{-4}$. The interpolation removes any ambiguity in the dynamics which might result from the choice of a fitting function and from the quality of the fitting, leaving us solely with the problem of the grid density, here chosen to be reasonably high for our purposes.

In the high energy range, we performed the dynamical simulation with a standard Time Dependent Wavepacket (TDWP) technique,[36–38] whereas for the low energy regime we employed a novel two-wavepacket method,[49] which has been recently implemented and tested in our group in 3D calculations of the reaction dynamics.[39] The latter method is designed to handle the dynamics at low energies, where the usual assumption of an initial wavepacket with only incoming

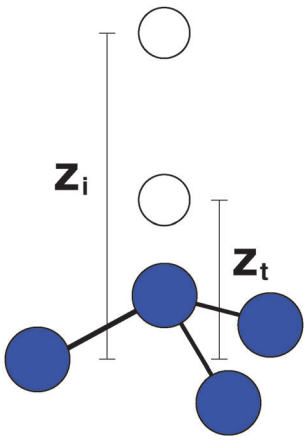

Fig. 1 Coordinate system: z_i and z_t are the distances of the incident and target H atoms from the surface. The z coordinate of the nearest carbon atom C_1 is either fixed in the puckered geometry ("sudden" model) or optimized at each position of the H atoms ("adiabatic" model).

momentum components breaks down. Briefly, in this approach two linearly independent, zero-momentum centered wavepackets are propagated in independent runs and the reaction probabilities are computed by properly combining the reaction amplitudes.[49] The latter are obtained by applying absorbing boundary conditions at the grid edges[50,51] (*i.e.* at large z_i and z_t), here imposed by means of the transmission-free absorbing potentials of Manolopoulos.[52]

With the present models, a time-*independent* quantum dynamical approach would be more convenient, especially at low energy, where such an approach proved indeed to be superior in efficiency and accuracy. However, in further developments of this work we aim at extending the dynamical model to include more degrees of freedom, up to eventually those of the lattice, and for such high-dimensional quantum problems (either exact or approximate) time-*dependent* wavepacket approaches are the only viable alternative.

3 Results and discussion

3.1 Potential energy surfaces

Our potential energy surfaces (see Fig. 2 for an overview) show that H_2 Eley–Rideal formation is a *non-activated*, exothermic reaction. No barrier could be found along the minimum energy path in any of the models considered in this work, at variance with previous cluster calculations with a coronene

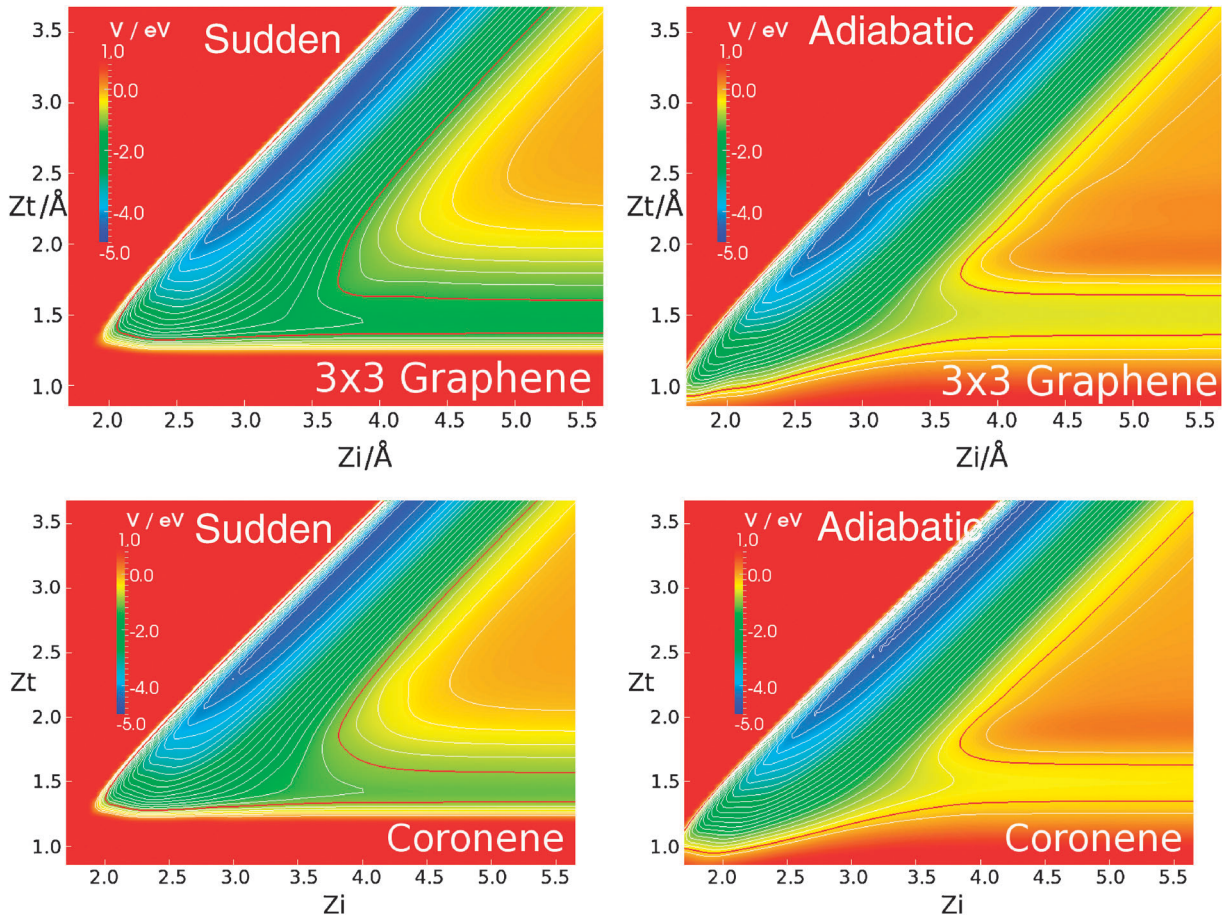

Fig. 2 Contour plots of the 3 × 3 periodic (top) and coronene (bottom) PES for the sudden (left) and the adiabatic (right) regimes. Potential is shown as a function of the height of the incident (z_i) and target (z_t) H atoms. The thick red line marks the energy of the vibrational ground state of the target H atom. Other contour lines have been plotted every 0.2 eV with respect to this vibrational energy. The zero of the energy corresponds to both the H atoms in the gas phase.

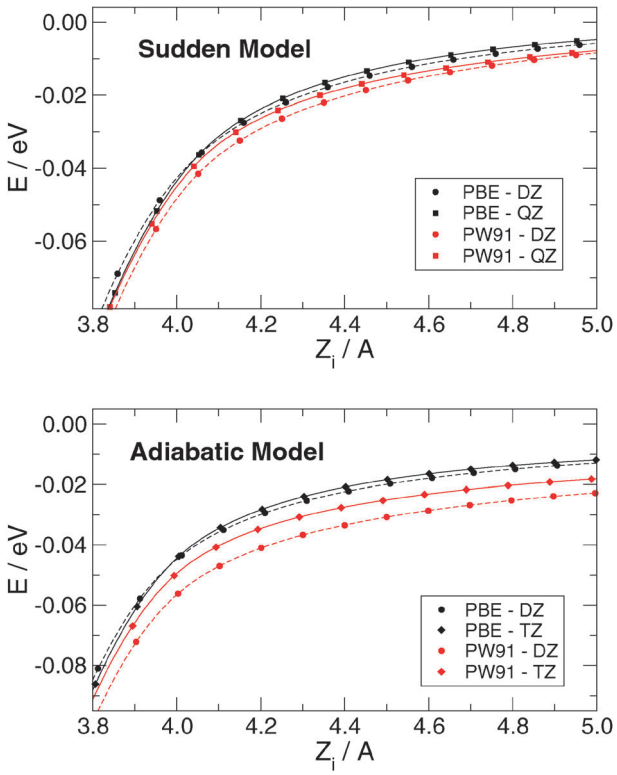

Fig. 3 Minimum energy path as a function of the height of the incident H atom, in the region where the presence of a barrier has been reported. We computed the energy with PW91 (in red) and PBE functionals (in black), for different Dunning's basis sets and both the dynamical regimes (sudden in the upper panel and adiabatic in the lower panel). We took as reference the energy of one H atom adsorbed on the surface and the other at infinite distance.

model which reported a barrier of 10 meV high in the entrance channel.[10,33] We systematically analyzed if such a tiny barrier could arise by using different functionals or basis sets, investigating the same coronene model in both dynamical regimes (sudden and adiabatic). In addition to the PBE functional adopted for the dynamics, we used the Perdew–Wang 1991 functional (PW91) used in ref. 33, both in conjunction with several Dunning's correlation-consistent basis-sets, up to quadruple-ζ. The results are reported in Fig. 3 as functions of the distance of the incident H atom from the surface, in the region where the barrier is expected. It is evident from the graph that the energy monotonically decreases from the asymptotic to the interaction region, leaving no room for a barrier at increasing basis-set level. Similarly, we exclude the presence of the barrier in the periodic models.

Apart from the barrier, the computed PES agree well with those computed by other authors. In both the adiabatic and the sudden models the entrance channel goes smoothly into the deep exit channel where the H_2 molecule forms. There are though differences between the two dynamical regimes. First of all, the adiabatic reaction is more exothermic than the other, since the puckering energy is released as the H_2 molecule leaves the surface. Secondly, in the adiabatic model the target H atom is allowed to get nearer to the surface, since the position of the carbon atom beneath is relaxed at each geometry. This determines a different *curvature* of the elbow potential which, as we will see in the following, plays a major role in determining the reaction dynamics. On the other hand, within the same dynamical regime, we hardly see any difference—at least at the energy scale of Fig. 2—between the surface models adopted; in particular, at this same scale, the results for the 2 × 2 periodic model (not reported) cannot be distinguished from those of the 3 × 3 periodic model. Differences only appear in the dynamical results.

3.2 Quantum dynamical results

Sudden models. Fig. 4 shows the results of the quantum dynamical calculations for the three sudden models. In this calculation the H target atom is initially in the vibrational ground state, the only one accessible in the relevant astrophysical conditions. Though the results for the low and high energy regimes are shown on different scales, there is a perfect matching between the curves where both results—ordinary wavepacket and two-wavepacket ones—are available.

In addition to the dynamical results obtained with the PES described above, we have reported previous results obtained with the London–Eyring–Polanyi–Sato (LEPS) potential fitted by Sha and Jackson to DFT periodic calculations on the 2 × 2 unit cell of graphene.[16] The calculations based on this LEPS potential describe the overall trend of the reaction probability but completely miss the fine structure that can be found in each of our calculations. This particular feature, already reported in the collinear calculations by Morisset *et al.*,[33] is due to Feshbach resonances, *i.e.* the formation of short lived vibrationally-excited species in asymptotically closed vibrational levels that become open at low energies.

This is supported by the comparison of the results for different vibrational states. The reaction probability for different initial states of the target H atom is plotted in Fig. 5 as a function of the total energy of the system, for the coronene and the 2 × 2 periodic models. The fine structures of the curves are similar: even if the peaks have different intensities, they are located at the same total energy values, corresponding to the energies of the resonant states. This structure is connected in a complex way to the vibrational states of the reaction channels and the peaks cluster near the energies of the vibrational levels of both the products and the reagents.

For each of the model potentials we considered, the reaction probability decreases with the collision energy, in agreement with previous calculations.[33,37,39] None of the PES give rise to a substantial reaction probability in the astrophysically relevant energy range (10^{-3}–10^{-2} eV)—except for a sharp resonance peak for the coronene PES located at 10^{-2} eV. As previously discussed, all the potential energy surfaces considered in the present study do not include any barrier in the entrance channel. Hence the results show that the low energy behavior is entirely due to quantum reflection.

In the high energy regime, the reaction probability for periodic and cluster models has a similar behavior, but the coronene potential gives a consistently higher reaction probability than the periodic ones, as evidenced by a comparison between the (smoothed) probability curves shown in Fig. 6 (upper panel) over a broad energy interval. Here smoothing has been accomplished by averaging each computed data in a

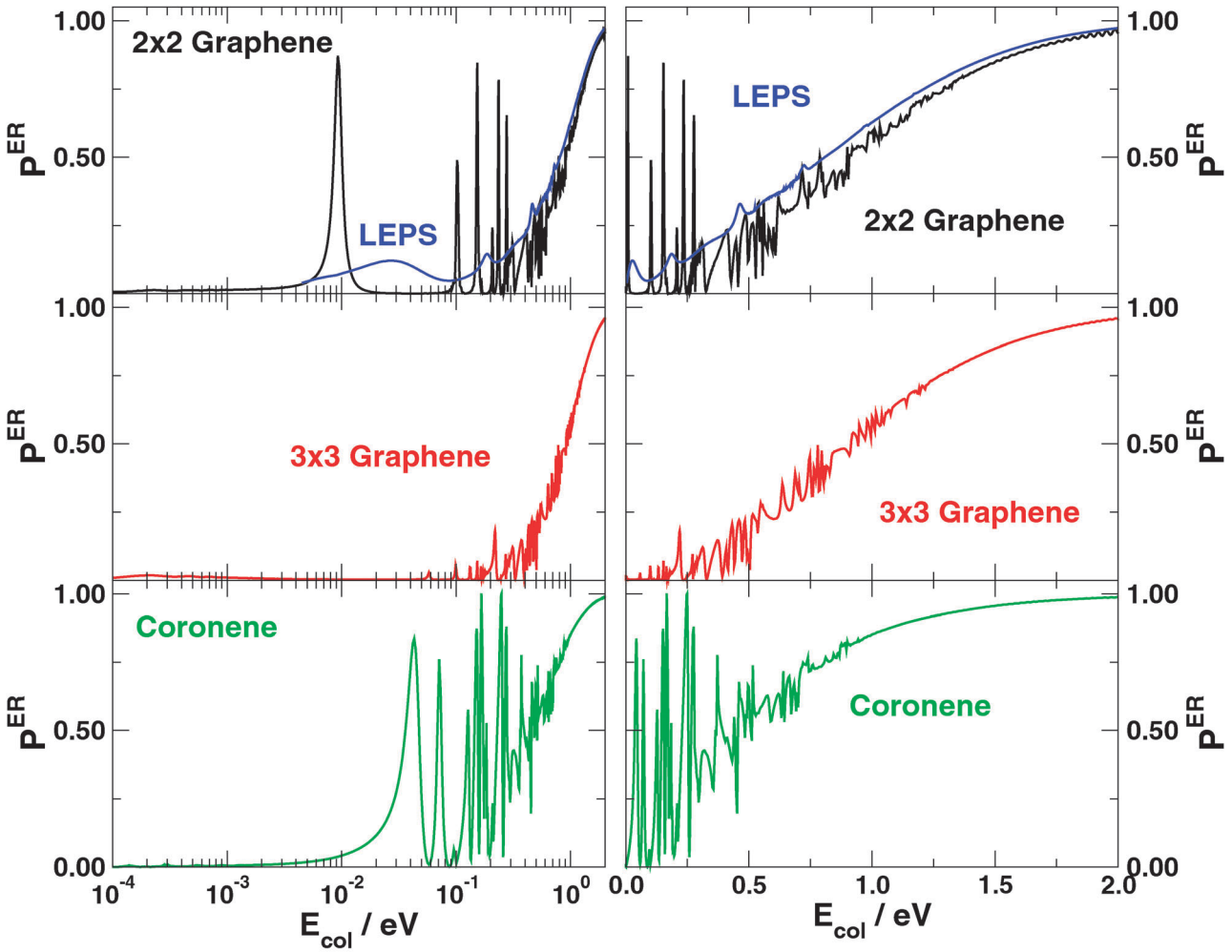

Fig. 4 Eley–Rideal, quantum reaction probability for the three sudden models with the reagents in the lowest vibrational state, for low energies (left panels, logarithmic scale from 10^{-4} eV $\approx$ 1 K to 1 eV $\approx$ 10 000 K) and at high energy on a linear scale (right panels). Green line for coronene, red for 3 $\times$ 3 graphene, black for 2 $\times$ 2 graphene, and blue for the LEPS PES of Sha and Jackson.[16]

narrow energy range to highlight the global behaviour which is masked by the resonance structure. The differences are due to a simple classical effect connected to the shape of the elbow in an otherwise simple, exoergic process. To investigate this point, we computed a set of classical trajectories (CT), which are reported in Fig. 7. These classical calculations were performed for the same sudden model, for coronene and the 2 $\times$ 2 periodic lattice models. At the beginning of these trajectories, the target H atom oscillates with an energy corresponding to its quantum ground state energy whereas the incident H atom approaches the surface with a kinetic energy of 0.5 eV in the collinear geometry. We sampled uniformly the initial position of the target atom to get insights into the reaction dynamics, as shown by plotting the reactive trajectories. No attempt was made to compute reaction probabilities from CT calculations, since the reliability of classical dynamics was already considered in our previous works.[36,37,39]

Most reactive trajectories share the very same "two bounce" mechanism. First the incident H atom collides with the target H atom and is pushed back. This corresponds to the first bounce of the trajectory, that is reflected by the H–H repulsion. In this first collision, some momentum is transferred between the two hydrogen atoms and the target atom moves towards the surface. Then the target atom collides with the surface which triggers the system to the products channel, where the two H atoms leave the surface in a highly excited vibrational state.

From the graph of Fig. 7 it is clear that in all the reactive trajectories the phase of the vibration of the target atom is similar. This suggests that the reaction mechanism is possible just for a particular interval of vibrational phases. For these vibrational phases, the system is reflected in the way described above by the two repulsive walls and driven to the products channel. In light of this, the difference between the periodic and the cluster models is that the phase interval of the reactive trajectories is broader for the coronene than the periodic model, suggesting that the former potential drives the hydrogen atoms towards the products in a more effective way.

Adiabatic models. The reaction probabilities for the different surface model in the adiabatic case are represented in Fig. 8 as functions of the kinetic energy of the incident atom, in the low and high energy regimes. As for the sudden case, the high energy results have been obtained with ordinary wavepacket techniques, whereas the low energy curves were computed with

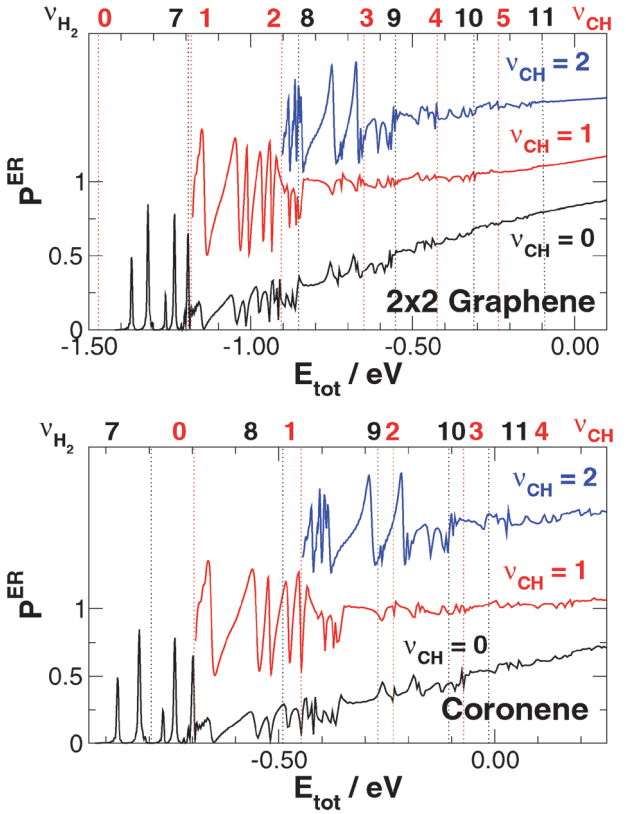

Fig. 5 Analysis of the resonance structure of the reaction probability for the 2 × 2 periodic and cluster sudden models. Reaction probabilities for a different initial vibrational state ν of the target H atom are reported as functions of the total energy. For convenience the curves for ν = 1, 2 have been shifted along the y axis. Dotted vertical lines mark the energies of the vibrational states of the reacting C–H bond (red) and product H_2 molecule (black). The energies of the first two vibrational quanta of the CH bond are: 0.29 eV and 0.56 eV (for the 2 × 2 graphene), 0.28 eV and 0.53 eV (for the coronene).

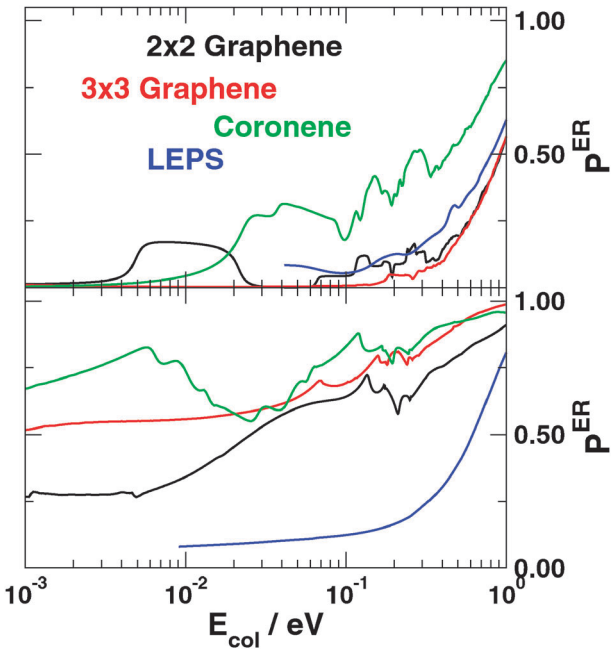

Fig. 6 Comparison between reaction probability, properly smoothed as described in the main text. Upper and lower panels for the sudden and adiabatic models.

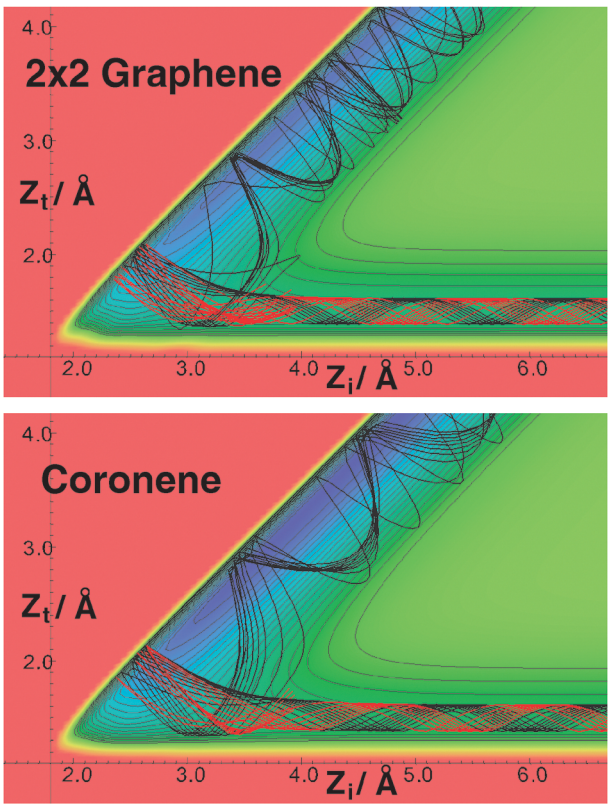

Fig. 7 Reactive (black) and non-reactive (red) classical trajectories for the 2 × 2 graphene and coronene sudden models are shown as a function of the incident (z_i) and target (z_t) heights from the surface.

the two-wavepacket approach. Also in this case, the target H atom is initially in the vibrational ground state.

Apart from the missing resonance structure, in this case the LEPS potential model fails to reproduce the overall trend of the curve and it highly underestimates the reaction probability for collision energy lower than 1.0 eV, thereby showing that the LEPS form is not flexible enough to fully describe the interaction potential in the adiabatic case.

In the high energy regime, all our surface models predict the reaction probability with a reasonable qualitative agreement. For collision energy below 0.5 eV, all the curves show sharp resonance peaks, that are particularly similar for the periodic models. In this energy range the reaction probability for coronene is higher than for the 3 × 3 graphene, that in turn is higher than for the 2 × 2 graphene, as evidenced in the smoothed data shown in the lower panel of Fig. 6.

In any case, the reaction probability increases up to 1.0 eV and then starts to decrease, due to the competing Collision Induced Desorption (CID) process.[37,38] In the energy range considered in this work, the CID channel is closed for the sudden model, but open for adiabatic models. In the latter case, in fact, the puckering energy is implicitly released during the dissociation of the target atom. The adiabatic models are approximately 0.9 eV more exothermic than the corresponding sudden ones and the CID channel for the adiabatic PES opens at lower collision energies.

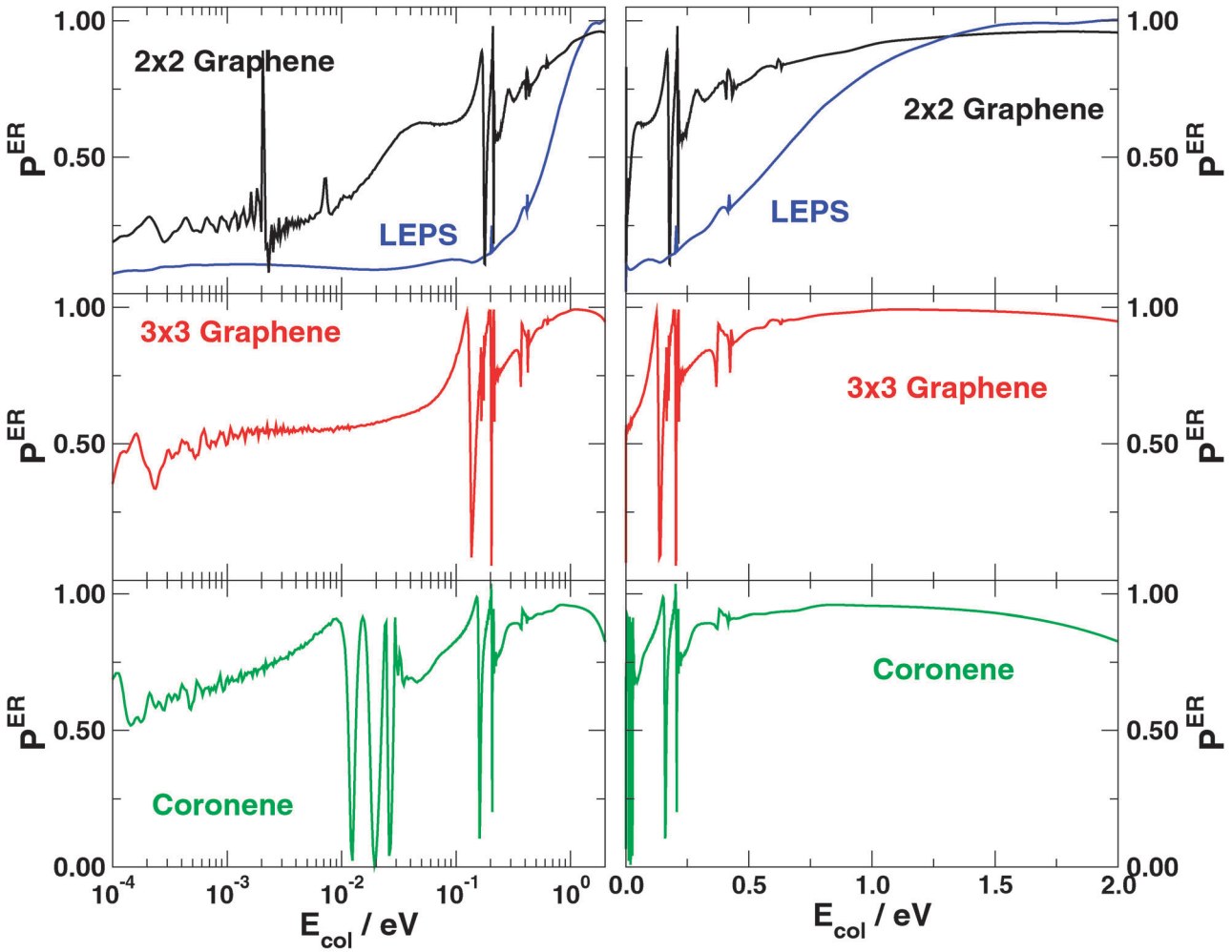

Fig. 8 Eley–Rideal, quantum reaction probability for the three adiabatic models with the reagents in the lowest vibrational state, for low energies (left panels, logarithmic scale from 10^{-4} eV $\approx$ 1 K to 1 eV $\approx$ 10 000 K) and at high energy on a linear scale (right panels). Green line for coronene, red for 3 × 3 graphene, black for 2 × 2 graphene, and blue for the LEPS PES of Sha and Jackson.[16]

Comparing the graphs in Fig. 4 and 8, we see that before saturation is reached, the reaction probability is much higher in the adiabatic limit than in the sudden one. This can be simply explained by computing some classical trajectories with the same initial conditions described above. The reactive trajectories for a collision energy of 0.5 eV in the case of the adiabatic 2 × 2 graphene PES are reported in Fig. 9. As can be seen, a similar "two-bounce" mechanism as the one described above is operating here. The difference here is the curvature of the surface–target atom repulsive wall that drives more effectively the system towards the products channel. Hence the implicit model of surface motion statically affects the reaction by changing the PES shape and making H_2 formation easier.

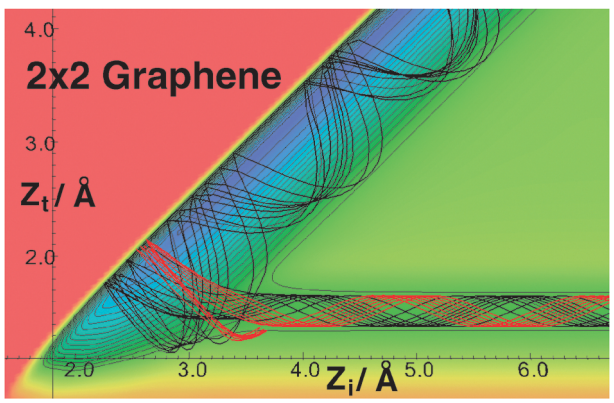

Fig. 9 Reactive (black) and non-reactive (red) classical trajectories for the 2 × 2 graphene adiabatic models are shown as a function of the incident (z_i) and target (z_t) heights from the surface.

In the low energy regime the reaction probability decreases with decreasing collision energy as in the sudden model. However, the reaction probability is different from zero in the astrophysically relevant low energy range. As for the high energy results, the reaction probability for coronene is higher than the probability for graphene, while among the periodic models, the 3 × 3 surface is more reactive than the 2 × 2 one. [Notice here that undulating features in the curve appear because of the presence of very sharp (long-lived) resonances which would require extremely long propagation times to be resolved.] In this energy range, the reflected fraction of the wavepackets is much smaller in the adiabatic regime than in the sudden one. This marked difference in the quantum

behaviour of the system is probably related to the curvature of the entrance channel: in the adiabatic models the potential changes smoothly from the entrance to the exit channel, whereas in the sudden case this transition is steeper and this increases the chance that the wavepacket is reflected back.

4 Conclusions

In this work, we computed quantum reaction probability for the collinear Eley–Rideal formation of H_2 over a broad range of collision energies, including the low energy regime relevant for the chemistry of the interstellar medium. In particular we investigated whether and how the dynamics of the system depends on the model adopted for the description of the surface. In light of this, we also addressed the problem of the presence of a tiny energy barrier in the entrance channel which was found by different authors.[10,33] We found that the minimum energy path is monotonically decreasing at any level of theory (in particular, basis-set size), and this strongly suggests that the title reaction is *barrierless*.

Concerning the dynamical results, we found that the results markedly depend on the choice of the model. While this is expected in the low energy regime, where the dynamics is very sensitive to the details of the potential, we found it to be true also at high collision energies. Under such circumstances, we found that when the same limiting approach is followed to describe the motion of the carbon atom—sudden or adiabatic—the results are qualitatively consistent but on quantitative grounds differences appear, the reaction probability being higher for the cluster model than for the periodic models. This is particularly true for the sudden models, but also holds to some extent for the adiabatic models. The reason of this discrepancy is the different shape of the entrance channel, that seems to play a major role in determining the reaction probability. Even a slight modification in the interaction potential—such as the difference between the 3 × 3 and coronene PESs—might drive the system more effectively towards the products, resulting in a higher reaction probability, see Fig. 6.

In agreement with previous studies, in the low energy regime we found that for all the models considered the reaction probability tends to zero with decreasing collision energy. This limiting behaviour can only be due to quantum reflection since, as stated above, our potential energy surfaces turn out to be barrierless. The efficiency of quantum reflection, on the other hand, is strongly dependent on the choice of the model, too. In the sudden regime, the whole wavepacket is reflected back to the entrance channel for any energy lower than 10^{-2} eV (100 K). If this were the case, we could reasonably assume that no reaction would take place in the astrophysical conditions. On the other hand, in the adiabatic regime, the probability vanishes only at much lower energies, thereby leaving open the possibility that a model including *dynamically* the motion of the carbon atom might give a reasonably sized probability in this energy regime. Also in this case, differences are found from model to model; for instance, the reaction probability for 3 × 3 graphene is 2–3 times higher than for 2 × 2 graphene in the 10^{-4}–10^{-2} eV range, see Fig. 8. From such discrepancy, we expect a similar factor for the corresponding reaction cross sections, when we move to three dimensional models.

In conclusion, moving to a less simplified and more realistic higher dimensional dynamical approach does require a careful choice of the substrate model used to build the PES. If the aim is to obtain the probabilities (cross-sections) for the reaction on graphite, then a large supercell approach seems to be necessary (maybe even larger than 3 × 3), especially in the limit where the carbon atom follows adiabatically the hydrogen evolution. In this respect, the above results suggest that modeling graphite (graphene) with a coronene molecule, despite many appealing features, is inadequate for investigating the present process. To this we add that while some features of the rigid-flat surface approximation are appropriate for this system (*e.g.* the rotational invariance of the interaction) the motion of the carbon atom needs likely to be explicitly included in the dynamical treatment (see also ref. 33). This defines a "minimal" 4D (quantum) model, and a corresponding interaction potential at the level outlined above. Work is currently in progress in order to set up such a model.

References

1 R. J. Gould and E. E. Salpeter, *Astrophys. J.*, 1963, **138**, 393.
2 D. Hollenbach and E. E. Salpeter, *J. Chem. Phys.*, 1970, **53**, 79–86.
3 D. Hollenbach and E. E. Salpeter, *Astrophys. J.*, 1971, **163**, 155.
4 J. M. Greenberg, *Surf. Sci.*, 2002, **500**, 793–822.
5 D. A. Williams and E. Herbst, *Surf. Sci.*, 2002, **500**, 823–837.
6 B. T. Draine, *Annu. Rev. Astron. Astrophys.*, 2003, **41**, 241–289.
7 M. Bonfanti, R. Martinazzo, G. F. Tantardini and A. Ponti, *J. Phys. Chem. C*, 2007, **111**, 5825–5829.
8 S. Morisset, F. Aguillon, M. Sizun and V. Sidis, *J. Chem. Phys.*, 2004, **121**, 6493–6501.
9 S. Morisset, F. Aguillon, M. Sizun and V. Sidis, *J. Chem. Phys.*, 2005, **122**, 194702.
10 D. Bachellerie, M. Sizun, F. Aguillon and V. Sidis, *J. Phys. Chem. A*, 2009, **113**, 108–117.
11 T. Zecho, A. Güttler, X. Sha, B. Jackson and J. Küppers, *J. Chem. Phys.*, 2002, **117**, 8486–8492.
12 A. Güttler, T. Zecho and J. Küppers, *Chem. Phys. Lett.*, 2004, **395**, 171–176.
13 A. Güttler, T. Zecho and J. Küppers, *Surf. Sci.*, 2004, **570**, 218–226.
14 T. Zecho, A. Güttler and J. Küppers, *Carbon*, 2004, **42**, 609–617.
15 L. Jeloaica and V. Sidis, *Chem. Phys. Lett.*, 1999, **300**, 157–162.
16 X. Sha and B. Jackson, *Surf. Sci.*, 2002, **496**, 318–330.
17 J. Kerwin, X. Sha and B. Jackson, *J. Phys. Chem. B*, 2006, **110**, 18811–18817.
18 Y. Ferro, F. Marinelli and A. Allouche, *Chem. Phys. Lett.*, 2003, **368**, 609–615.
19 J. Kerwin and B. Jackson, *J. Chem. Phys.*, 2008, **128**, 084702.
20 S. Casolo, O. M. Løvvik, R. Martinazzo and G. F. Tantardini, *J. Chem. Phys.*, 2009, **130**, 054704.
21 L. Hornekær, Ž. Šljivančanin, W. Xu, R. Otero, E. Rauls, I. Stensgaard, E. Lægsgaard, B. Hammer and F. Besenbacher, *Phys. Rev. Lett.*, 2006, **96**(15), 156104.
22 L. Hornekær, E. Rauls, W. Xu, Ž. S Šljivančanin, R. Otero, I. Stensgaard, E. Lægsgaard, B. Hammer and F. Besenbacher, *Phys. Rev. Lett.*, 2006, **97**(18), 186102.
23 L. Hornekær, W. Xu, R. Otero, E. Lægsgaard and F. Besenbacher, *Chem. Phys. Lett.*, 2007, **446**, 237–242.
24 A. Andree, M. L. Lay, T. Zecho and J. Küppers, *Chem. Phys. Lett.*, 2006, **425**, 99–104.
25 N. Rougeau, D. Teillet-Billy and V. Sidis, *Chem. Phys. Lett.*, 2006, **431**, 135–138.
26 A. J. H. M. Meijer, A. J. Farebrother, D. C. Clary and A. J. Fisher, *J. Phys. Chem. A*, 2001, **105**, 2173–2182.
27 A. J. H. M. Meijer, A. J. Farebrother and D. C. Clary, *J. Phys. Chem. A*, 2002, **106**, 8996–9008.
28 A. J. H. M. Meijer, A. J. Fisher and D. C. Clary, *J. Phys. Chem. A*, 2003, **107**, 10862–10871.

29 M. Rutigliano, M. Cacciatore and G. D. Billing, *Chem. Phys. Lett.*, 2001, **340**, 13–20.
30 M. Rutigliano and M. Cacciatore, *ChemPhysChem*, 2008, **9**, 171–181.
31 B. Jackson and D. Lemoine, *J. Chem. Phys.*, 2001, **114**, 474–482.
32 S. Morisset, F. Aguillon, M. Sizun and V. Sidis, *Phys. Chem. Chem. Phys.*, 2003, **5**, 506–513.
33 S. Morisset, F. Aguillon, M. Sizun and V. Sidis, *J. Phys. Chem. A*, 2004, **108**, 8571–8579.
34 D. Bachellerie, M. Sizun, F. Aguillon, D. Teillet-Billy, N. Rougeau and V. Sidis, *Phys. Chem. Chem. Phys.*, 2009, **11**, 2715–2729.
35 M. Sizun, D. Bachellerie, F. Aguillon and V. Sidis, *Chem. Phys. Lett.*, 2010, **498**, 32–37.
36 R. Martinazzo and G. F. Tantardini, *J. Phys. Chem. A*, 2005, **109**, 9379–9383.
37 R. Martinazzo and G. F. Tantardini, *J. Chem. Phys.*, 2006, **124**, 124702.
38 R. Martinazzo and G. F. Tantardini, *J. Chem. Phys.*, 2006, **124**, 124703.
39 S. Casolo, R. Martinazzo, M. Bonfanti and G. F. Tantardini, *J. Phys. Chem. A*, 2009, **113**, 14545–14553.
40 M. Persson and B. Jackson, *J. Chem. Phys.*, 1995, **102**, 1078–1093.
41 D. Lemoine and B. Jackson, *Comput. Phys. Commun.*, 2001, **137**, 415–426.
42 J. P. Perdew, K. Burke and M. Ernzerhof, *Phys. Rev. Lett.*, 1996, **77**, 3865–3868.
43 J. P. Perdew, K. Burke and M. Ernzerhof, *Phys. Rev. Lett.*, 1997, **78**, 1396.
44 T. H. Dunning, *J. Chem. Phys.*, 1989, **90**, 1007–1023.
45 M. J. Frisch, G. W. Trucks, H. B. Schlegel, G. E. Scuseria, M. A. Robb, J. R. Cheeseman, J. J. A. Montgomery, T. Vreven, K. N. Kudin, J. C. Burant, J. M. Millam, S. S. Iyengar, J. Tomasi, V. Barone, B. Mennucci, M. Cossi, G. Scalmani, N. Rega, G. A. Petersson, H. Nakatsuji, M. Hada, M. Ehara, K. Toyota, R. Fukuda, J. Hasegawa, M. Ishida, T. Nakajima, Y. Honda, O. Kitao, H. Nakai, M. Klene, X. Li, J. E. Knox, H. P. Hratchian, J. B. Cross, V. Bakken, C. Adamo, J. Jaramillo, R. Gomperts, R. E. Stratmann, O. Yazyev, A. J. Austin, R. Cammi, C. Pomelli, J. W. Ochterski, P. Y. Ayala, K. Morokuma, G. A. Voth, P. Salvador, J. J. Dannenberg, V. G. Zakrzewski, S. Dapprich, A. D. Daniels, M. C. Strain, O. Farkas, D. K. Malick, A. D. Rabuck, K. Raghavachari, J. B. Foresman, J. V. Ortiz, Q. Cui, A. G. Baboul, S. Clifford, J. Cioslowski, B. B. Stefanov, G. Liu, A. Liashenko, P. Piskorz, I. Komaromi, R. L. Martin, D. J. Fox, T. Keith, M. A. Al-Laham, C. Y. Peng, A. Nanayakkara, M. Challacombe, P. M. W. Gill, B. Johnson, W. Chen, M. W. Wong, C. Gonzalez and J. A. Pople, *GAUSSIAN 03 (Revision C.02)*, Gaussian, Inc., Wallingford, CT, 2004.
46 G. Kresse and J. Furthmüller, *Comput. Mater. Sci.*, 1996, **6**, 15.
47 P. E. Blöchl, *Phys. Rev. B: Condens. Matter*, 1994, **50**, 17953–17979.
48 G. Kresse and D. Joubert, *Phys. Rev. B: Condens. Matter Mater. Phys.*, 1999, **59**, 1758–1775.
49 R. Martinazzo and G. F. Tantardini, *J. Chem. Phys.*, 2005, **122**, 094109.
50 D. Neuhasuer and M. Baer, *J. Chem. Phys.*, 1989, **90**, 4351–4355.
51 D. Neuhauser and M. Baer, *J. Chem. Phys.*, 1989, **91**, 4651–4657.
52 D. E. Manolopoulos, *J. Chem. Phys.*, 2002, **117**, 9552–9559.

